Received: 23 December 2021 | Accepted: 18 May 2022

DOI: 10.1111/gcb.16313

Global Change Biology WILEY

RESEARCH ARTICLE

New tree-level temperature response curves document sensitivity of tree growth to high temperatures across a US-wide climatic gradient

Joséphine Gantois[1,2]

[1]Institute for Resources, Environment and Sustainability, University of British Columbia, Vancouver, British Columbia, Canada

[2]School of International and Public Affairs, Columbia University, New York, New York, USA

Correspondence
Joséphine Gantois, Institute for Resources, Environment and Sustainability, University of British Columbia, Vancouver, British Columbia, Canada.
Email: josephine.gantois@ubc.ca

Abstract

Temperature is a key climate indicator, whose distribution is expected to shift right in a warming world. However, the high-temperature tolerance of trees is less widely understood than their drought tolerance, especially when it comes to sub-lethal impacts of temperature on tree growth. I use a large data set of annual tree ring widths, combined with a flexible degree day model, to estimate the relationship between temperature and tree radial growth. I find that tree radial growth responds non-linearly to temperature across many ecoregions of the United States: across temperate and/or dry ecoregions, spring–summer temperature increases are beneficial or mostly neutral for tree growth up to around 25–30°C in humid climates and 10–15°C in dry climates, beyond which temperature increases suppress growth. Thirty additional degree days above the optimal temperature breakpoint lead to an average decrease in tree ring width of around 1%–5%, depending on ecoregions, seasons, and inclusion or exclusion of temperature-mediated drought impacts. High temperatures have legacy effects across a 5-year horizon in dry ecoregions, but none in the temperate-humid South-East or among temperature-sensitive trees. I find limited evidence that trees acclimatize to high temperatures within their lifetime: local variation in early exposure to high temperatures, which stems from local variation in the timing of tree birth, does not significantly impact the response to high temperatures, although temperature-sensitive trees acquire some heightened sensitivity from early exposure. I also find some evidence that trees adapt to high temperatures in the long run: across humid ecoregions of the United States, high temperatures are 40% less harmful to tree growth, where their average incidence is one standard deviation above average. Overall, these results highlight the strength of a new methodology which, applied to representative tree ring data, could contribute to predicting forest carbon uptake potential and composition under global change.

KEYWORDS
climate change, ecoregion patterns, high-temperature acclimatization, high-temperature adaptation, high-temperature tolerance, non-linear impacts, radial tree growth, thermal performance curve, tree ring

1 | INTRODUCTION

Ongoing warming is manifesting globally, with the full distribution of temperature progressively shifting to the right (IPCC, 2021; Pachauri et al., 2014). Warming is already affecting forest carbon uptake (Allen et al., 2010), with significant projected consequences on the carbon cycle (Frank et al., 2015). However, there remain large uncertainties about future rates of forest carbon sequestration (Sitch et al., 2008; Winkler et al., 2019). While there is growing evidence about the impact of drought on tree mortality (DeSoto et al., 2020) and tree growth (D'Orangeville et al., 2018), the impact of temperature on tree growth, and particularly the sub-lethal impact of high temperatures, those that exceed the thermal optimum, is less widely understood (Allen et al., 2015; Breshears et al., 2021). Growth suppression induced by high temperatures, while less severe than mortality, is likely to matter for future rates of carbon sequestration (Brzostek et al., 2014) and might enhance the sensitivity of trees to other stressors like drought or pests (Heilman et al., 2022; McKenzie et al., 2008). In this context, it is critical to resolve how tree growth responds to temperature. It is particularly important to elucidate potential non-linearities across the temperature distribution (Evans et al., 2022) and to identify the impact of high temperatures specifically, to fully capture the impact of ongoing shifts in the temperature distribution.

This temperature response is likely to be heterogeneous across forests. Not only are species and traits likely to influence tree growth sensitivity to temperature (Bréda et al., 2006; Clark, 2016), but there is growing evidence that local conditions shape species-specific and trait-specific responses to the environment (Anderegg et al., 2015; Charney et al., 2016; D'Orangeville et al., 2018; Klesse et al., 2020; Restaino et al., 2016), to the point that sites more than species drive differences in tree growth (Fritts, 1974; Martin-Benito & Pederson, 2015). Addressing spatial heterogeneity in the temperature response of tree growth across different climates and environments might be key to gain precise insights into the growth implications of changes in temperature.

Another key dimension shaping temperature impacts on tree growth is the capacity of trees to adapt to temperature, and especially to stressful high temperatures. Such adaptability could manifest via different mechanisms and over different time horizons. Tree growth could rebound from stressful temperature events by overshooting regular growth rates in the following years. This could be the result of strategies such as prioritizing storage over growth in a stressful year (Fatichi et al., 2014), or reallocating biomass to non-cambium structures like leaves to increases future rates of carbon uptake (Poyatos et al., 2013). This suggests looking at the long-term impacts of high-temperature exposure. In addition, the potential for trees to acclimatize to high temperatures within their lifetime via phenotypic plasticity in their temperature response, is likely to influence tree growth sensitivity, and play a crucial role in shaping tree persistence and forest composition under rapid climate change, given the slower pace of evolutionary and migratory responses (Gratani, 2014). There is evidence of short-run acclimation to warming in experimental settings (Nievola et al., 2017), focusing on photosynthesis (Gunderson et al., 2010; Kattge & Knorr, 2007; Wang et al., 1996), respiration (Smith & Dukes, 2013), and the timing of bud burst (Montgomery et al., 2020). However, there is no indication that ecosystem-level net gross primary productivity has acclimatized to the recent warming trend (Huang et al., 2019). The potential for tree growth to acclimatize to high temperatures throughout their lifetime is essentially unknown. Finally, trees are likely to adapt to their local environment as a result of long-term evolutionary forces. There is some within-species evidence that tree growth response to mean annual temperature adapts to the long-term local climate (Canham et al., 2018). However, evidence on the evolution of high heat tolerance is scarce, and restricted to leaf-level and ecosystem-level carbon exchange processes (Huang et al., 2019; O'sullivan et al., 2017).

Reducing uncertainties regarding tree growth sensitivity and adaptability to shifting temperature distributions requires observations with a large spatiotemporal scope. Tree ring data provide a direct record of radial tree growth, which covers a large number of years and locations. The temporal depth of these data provides local variation in temperature realizations, which helps to identify the detailed temperature response of tree growth. The large spatial coverage helps to average out statistically the influence of other growth factors like soil type or competition, and allows to explore heterogeneity in the temperature response across locations. In order to fully take advantage of this rich variation, I adopt a joint model approach (Schofield et al., 2016; Steinschneider et al., 2017), also referred to as an aggregate model approach (Cook, 1987; Klesse et al., 2020), where the influence of different growth factors, such as age, climate, local environment and idiosyncratic factors, is simultaneously estimated. I combine this approach with tools from econometrics to identify the causal impact of temperature on tree growth, to exploit temporal variation in short-to-medium-term exposure to high temperatures, which can shed light on acclimatization, and to exploit spatial variation in long-term climatic differences in high-temperature exposure, which can shed light on adaptation.

Documenting tree growth sensitivity and adaptability to shifting temperature distributions also requires to accurately estimate non-linear impacts of temperature on tree growth. Such non-linear responses to temperature have been documented experimentally for different physiological processes underlying growth, such as net photosynthesis (Kattge & Knorr, 2007; Lloyd & Farquhar, 2008; Medlyn et al., 2002; Waring & Running, 2010), nitrogen fixation (Bytnerowicz et al., 2022), and the timing of cambial reactivation (Begum et al., 2018). However, tree growth is a complex combination of carbon assimilation and other processes, such that high temperatures might start to inhibit tree growth at lower levels compared to carbon exchange processes (Fatichi et al., 2014), which calls for a more precise estimation of growth-specific non-linearities. In addition, there is a tradeoff between using fine-scale weather data, which can be used to detect non-linearities and breakpoints in the effect of temperature on tree growth, and relying on temporally coarse annual tree ring data to achieve a large spatiotemporal scope. Large-scale studies documenting temperature impacts on tree growth rely on annual temperature aggregates, such as average temperature, or maximum temperature over one of more months of the growing season (Babst et al., 2019; Charney et al., 2016; Heilman

et al., 2022; Klesse et al., 2020; Restaino et al., 2016), to match the temporal resolution of tree ring data. This type of aggregation masks within-year fluctuations, including the intensity and severity of high-temperature events, which dilutes the true temperature response if it is non-linear, and prevents the estimation of a precise temperature response curve across the full range of possible temperatures. Following Schlenker and Roberts (2009), I aggregate half-hourly temperature data at the annual level using a cumulative degree day formulation: each degree experienced during the year contributes to that year's growth, and can have a different impact on growth depending on the temperature bracket it belongs to. This framework is common in agronomic studies. It has been used to estimate the temperature response curve of different crops, and highlight their sensitivity to high temperatures especially (Schlenker & Roberts, 2009). It is also present in tree-specific studies: growing degree days have been used to predict the timing of cambial reactivation at the beginning of the growing season (Begum et al., 2018), and they have been reconstructed from historical tree ring data at Northern latitudes (Jacoby et al., 1985).

Here, I test the hypothesis that tree radial growth responds non-linearly to temperature, such that temperature enhances tree radial growth up to an "optimal" temperature level, lower than the critical thermal limit of trees, beyond which temperature decreases growth. I document spatial heterogeneity in that response, and trait heterogeneity to some extent. I then exploit those new temperature response curves to document the legacy effects of high temperatures, the extent of medium-run acclimatization of tree growth to high temperatures—based on differences in early life weather exposure to high temperature, among trees living in the same location—, and the extent to which spatial heterogeneity in the temperature response denotes adaptation to the local climate, via a lower impact of high temperature where those are more frequently experienced.

To this end, I exploit tree ring data from 51,859 tree cores, spanning six large ecoregions of the United States and years 1903 to 2016. I match them to half-hourly temperature data, aggregated into total annual or seasonal degree days, to match the annual resolution of tree ring data while preserving information on within-year fluctuations in temperature. I adopt a statistical modeling approach that seeks to isolate the causal impact of temperature on tree radial growth, and allows for a non-linear impact of temperature on growth.

2 | MATERIALS AND METHODS

2.1 | Tree growth data

Data on tree radial growth come from the International Tree-Ring Data Bank (ITRDB; https://www.ncei.noaa.gov/access/paleo-search/, February 2019). I extract all records from that public repository, and filter them to focus on the contiguous United States and years 1903 to 2016 (Figure 1a,b). Total annual ring width, which is the most

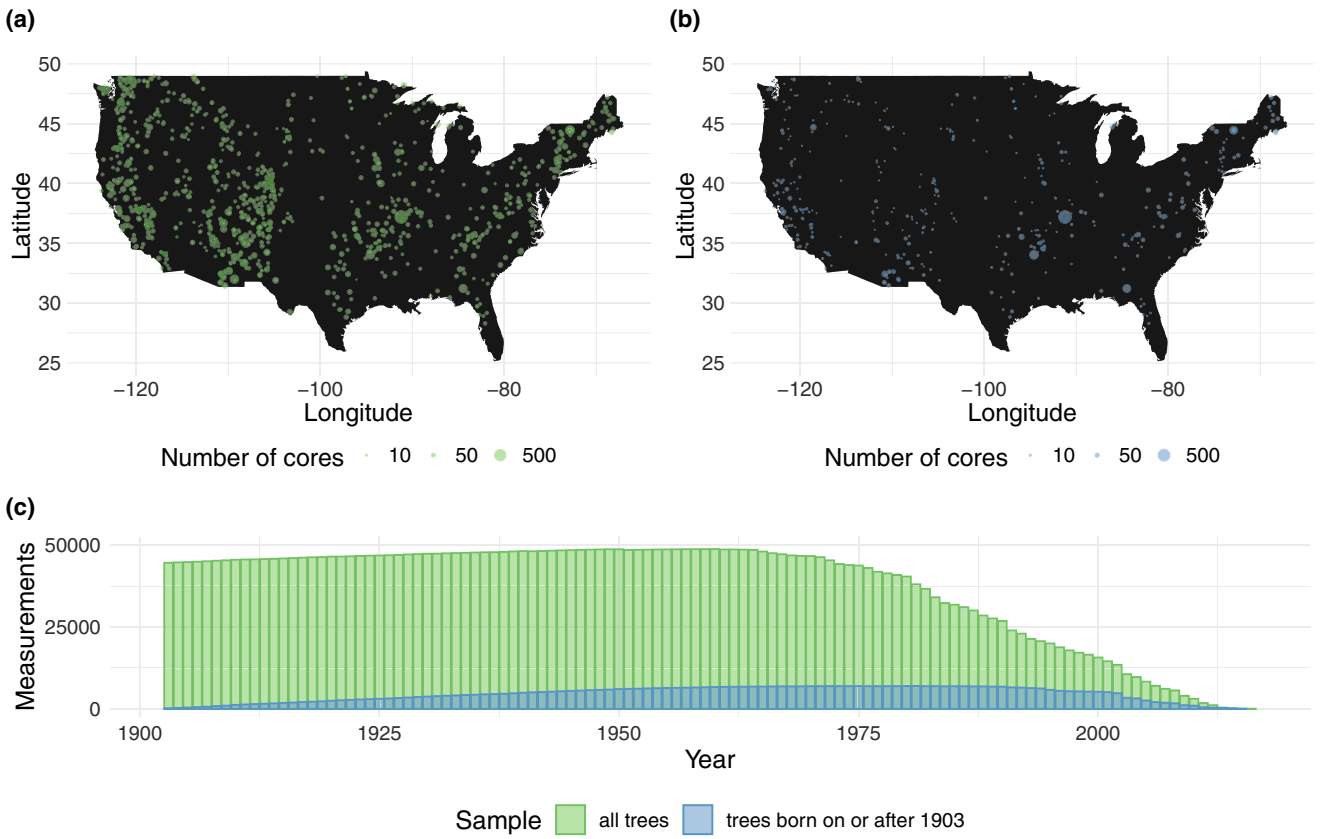

FIGURE 1 (a, b) Location of tree ring sequences and (c) frequency of measurements over time. Circle size indicates the number of tree cores sampled at each location. (a) All trees. (b) Trees born on or after 1903. [Colour figure can be viewed at wileyonlinelibrary.com]

consistently reported measurement, is my metric of tree growth. Although some data cleaning, primarily related to formatting issues, is necessary to make this public repository exploitable and reliable (Supplemental Materials and Methods 2.1 in Appendix S1), I do not standardize measurements prior to analysis or create site-level chronologies. One advantage of using an aggregate model is that standardization can be performed jointly with model estimation (Schofield et al., 2016; Steinschneider et al., 2017), and site structure can be explicitly modeled. In total, I use 4,241,428 ring width measurements from 51,859 tree cores across 1284 locations (the final data are available from dryad, Gantois, 2022). For each tree core, measurements usually extend from the outermost ring under the bark to, or very near, the pith of the tree, although there can be gaps due to true missing rings or measurement issues. The average length of a tree core time series is 82 years. A subset of the data, restricted to trees born on or after 1903, is used to test the acclimatization hypotheses (Figure 1b,c). These hypotheses require characterizing individual trees' weather history from birth, and weather data are available from 1903 onwards, hence the data restriction.

The ITRDB does not represent a regionally representative sample of trees. It primarily contains data on trees used for reconstruction of climatic variables in the past, which are precisely selected for their responsiveness to climate. In fact, the climate sensitivity of these trees has been estimated to be about 50% higher than regional forest climate sensitivity in the South-West of the United States, based on a comparison with tree ring data from the Forest Inventory and Analysis program (Klesse et al., 2018, although see Babst et al., 2019). This does not affect the relevance of constructing temperature response curves for those climate-sensitive trees, or of testing the extent of their temperature acclimatization and adaptation. However, this prevents extrapolation to other tree species or forest-level dynamics, and might impact comparisons across regions if sampling strategies vary by location.

2.2 | Weather data

Temperature and precipitation data come from the "Parameter-Elevation Regressions on Independent Slopes Model" (PRISM), which covers the contiguous United States at a 4 km resolution. Precipitation is available as monthly totals. For temperature, monthly minima and maxima are downscaled at the daily level, using a robust methodology first implemented by Schlenker and Roberts (2006) and updated in 2020. It follows a three-step process: first, monthly data in each PRISM grid cell are regressed on monthly averages from the closest 10 instrumental stations that have continuous coverage (the R^2 of this model is 0.999); second, missing daily values at those stations are interpolated from neighboring stations with non-missing values; third, the relationship estimated in the first step is used to infer daily values at each grid cell from daily values at the station level. From these daily maximum and minimum temperature data, the within-day temperature distribution is extrapolated by fitting a sinusoidal curve. The end-product is half-hourly temperature data, across 1900–2016. Given the extent of within-day temperature fluctuations, this last step allows to capture high-temperature occurrences much more precisely than when using daily average temperature, or monthly aggregates. A key characteristic of the PRISM interpolation model is that it takes elevation into account, in addition to reproducing gradients caused by temperature inversions, rain shadows or coastal effects. Tree ring data cover large elevation ranges, especially in the South-West of the United States, which makes PRISM particularly adapted to this setting.

The total impact of temperature on tree growth combines direct effects like temperature-induced acceleration of enzymatic processes, and indirect effects via coupled factors like vapor pressure deficit and soil moisture. To test how much the temperature response of tree growth is driven by temperature-mediated drought conditions, I use data from the standardized precipitation-evapotranspiration index (SPEI) database (Beguería et al., 2014). The SPEI index captures deviations from the local average water balance (precipitation net of potential evapotranspiration) at different timescales. I use the 1-month and 3-month SPEI to capture short-term drought conditions, and the 12-month SPEI to capture medium-term drought conditions, which reflect both sustained atmospheric drought conditions, and slower evolving soil moisture conditions. I choose this index over other drought indices for its independence of tree ring data, ability to capture ecological impacts, and flexibility of timescales for capturing a priori complex and potentially heterogeneous impacts across tree species and regions (Bhuyan et al., 2017; Vicente-Serrano et al., 2013).

2.3 | Ecoregion data

Tree ring data from the continental US are split into ecoregions based on the Köppen-Geiger climate classification, which is driven by differences in vegetation types across locations (Kottek et al., 2006). Each ecoregion is identified by a three-letter code: the first letter denotes the main climatic group (B for dry, C for temperate, and D for continental), the second denotes the precipitation pattern (W for desert, S for steppe, f for fully humid, s for summer dry), and the third denotes the temperature pattern (k for cold arid, a for hot summer, b for warm summer, c for cool summer). I restrict the study of ecoregion patterns to ecoregions in which tree ring sites span at least 35 different PRISM grid cells (Figure 2, Figure S1). This safeguards against low levels of spatial variation in the temperature predictors, since temperature varies by PRISM grid cell, and it excludes less than 10% of the data. Two ecoregions are characterized by a dry climate: BSk in the South-West, and Csb along the Western coast. All other ecoregions are characterized as "fully humid" ("f"), with varying levels of summer temperatures ("a," "b," or "c," in decreasing order of heat). The spatial distribution of the most frequently sampled tree species closely follows the spatial distribution of ecoregions (Figure S2). In the ITRDB data, species selection tends to be influenced by the local climate, and often, a single tree species is sampled at a given location. As a result, in most ecoregions, tree

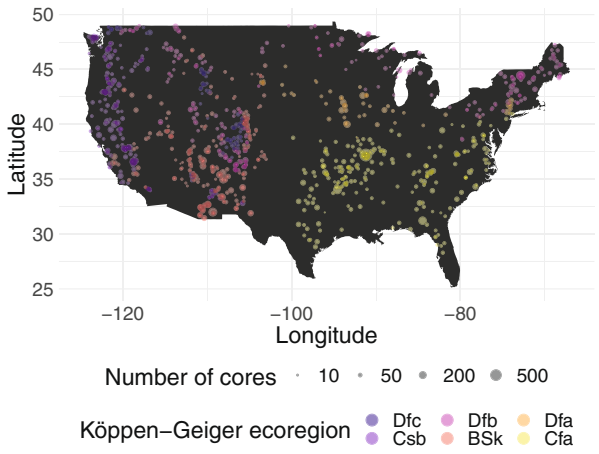

FIGURE 2 Location of tree ring sequences, by Köppen-Geiger ecoregion. Circle size indicates the number of tree cores sampled at each location. [Colour figure can be viewed at wileyonlinelibrary.com]

ring data are disproportionately dominated by a single tree species (Figure S3), which prevents looking at heterogeneous temperature impacts across species in addition to ecoregions.

2.4 | Temperature response curve: Baseline model, by ecoregion

2.4.1 | Piecewise linear response to temperature

The relationship between ring width and temperature is modeled using a piecewise linear function with a single breakpoint (Table 1, model 1). This breakpoint allows for a non-linear impact of temperature, where temperature increases can have a different impact on ring width below and above a certain temperature level. In particular, it can help isolate the impact of temperature increases at high-temperature levels. The temperature level used as a breakpoint is not imposed based on prior knowledge; it is selected flexibly among all degree integers in the [1–40°C] range, using a 10-fold cross-validation procedure that uses random sets of years held out from training to measure each model's predictive performance. The integer that gives the lowest root mean squared error on average across all folds is selected as the optimal temperature breakpoint. The model relates tree ring width, which is log transformed to reflect its lognormal distribution, with temperature, which is captured by two annual aggregates: total degree days below the optimal temperature breakpoint and total degree days above the optimal temperature breakpoint. Both degree day variables are summed across a non-calendar year starting in the previous September and ending in August of the year of ring formation. This reflects patterns of growth phenology characteristic of many temperate trees (D'Orangeville et al., 2022; Etzold et al., 2022). An important assumption underlies this non-linear degree day model: temperature effects on tree growth are cumulative over time and annual tree growth is proportional to total exposure.

The focus of this study is on the estimation of the causal impact of temperature on ring width. Accordingly, the goal is not to maximize overall predictive performance; rather, it is to control for growth factors that are correlated with temperature and could confound the impact estimate, unless they represent pathways through which temperature impacts growth. For instance, precipitation is likely a confounding factor, as it impacts both temperature via solar radiation, and tree growth via atmospheric and soil moisture. Soil moisture on the other hand could be a non-confounding pathway: after controlling for precipitation, if the leftover impact of soil moisture on growth is purely temperature driven, then this covariate will be a channel of impact rather than a confounder (Fritts, 2012, figure 5.8). The model equation is as follows, where y_{ct} is log ring width from tree core c, formed in year t, and located in PRISM grid cell s:

$$y_{ct} = \alpha_c + \beta_1 \underset{[0,X],\text{annual}}{\text{low\_degree\_days}_{st}} + \beta_2 \underset{(X,+\infty),\text{annual}}{\text{high\_degree\_days}_{st}} + \delta_1 \text{precip}_{st} + \delta_2 \text{precip}^2{}_{st} + \delta_3 \text{age}_{ct} + \varepsilon_{ct}$$

$$\underset{[0,X],\text{annual}}{\text{low\_degree\_days}_{st}} = \left[\sum_{\substack{\text{days } d \\ \text{from Sept } t-1 \\ \text{to Aug } t}} \frac{1}{48} \left(\sum_{\substack{\text{half-hour } h \\ \text{in day } d}} \max(0, \min(T_{sh}, X)) \right) \right]$$

$$\underset{(X,+\infty),\text{annual}}{\text{high\_degree\_days}_{st}} = \left[\sum_{\substack{\text{days } d \\ \text{in year } t}} \frac{1}{48} \left(\sum_{\substack{\text{half-hour } h \\ \text{in day } d}} \max(0, T_{sh} - X) \right) \right]$$

Following terminology used in econometrics, tree core fixed effects α_c account for time-invariant characteristics of a tree that might be correlated with both temperature and growth, such as soil quality, baseline climate, or species-specific average growth rate. Including those fixed effects is equivalent to including a dummy variable for each tree core identifier. It is also equivalent to demeaning both outcome and predictor variables at the tree core level. Tree core fixed effects imply that the model exploits temporal variation in temperature at the tree core level, and does not rely on spatial variation in baseline temperatures, which helps isolate the causal impact of temperature on tree growth. Variables precip_{st} and $\text{precip}^2{}_{st}$ capture a quadratic influence of total annual precipitation, which allows for a different impact of very low and very high precipitation levels. This controls for unusually wet or dry years, which could be correlated with temperature, and have a documented impact on tree ring width across the United States (George, 2014). The term age_{ct} is a linear control in tree age, which allows for a linearly decreasing log growth rate over a tree's lifetime, similar to a traditional form of age standardization (Schofield et al., 2016). Following terminology used in econometrics, standard errors are clustered at a 2° grid cell level, in the sense that

TABLE 1 List of models estimated and corresponding interpretation

Model number	Short description	Equation	Breakpoint identification	Core interpretation
Temperature response curve, by ecoregion				What is the causal impact of temperature on tree radial growth?
1	Annual (September–August) response	$y_{ct} = \alpha_c + \beta_1 \underset{[0,X],\text{annual}}{\text{low\_degree\_days}_{st}} + \beta_2 \underset{(X,+\infty),\text{annual}}{\text{high\_degree\_days}_{st}} + \delta_1 \text{precip}_{st} + \delta_2 \text{precip}^2{}_{st} + \delta_3 \text{age}_{ct} + \varepsilon_{ct}$	X is selected in [1–40°C] using 10-foldcross-validation	β_1: impact of an additional degree day below X (experience anytime of year) on log annual growth β_2: impact of an additional degree day above X (experienced anytime of year) on log annual growth
2	Seasonal (AMJJA) response	$y_{ct} = \alpha_c + \beta_1 \underset{[0,X],\text{AMJJA}}{\text{low\_degree\_days}_{st}} + \beta_2 \underset{(X,+\infty),\text{AMJJA}}{\text{high\_degree\_days}_{st}} + \delta_1 \text{precip}_{st} + \delta_2 \text{precip}^2{}_{st} + \delta_3 \text{age}_{ct} + \varepsilon_{ct}$	Same as above	β_1: impact of an additional degree day below X (experienced during AMJJA) on log annual growth β_2: impact of an additional degree day above X (experienced during AMJJA) on log annual growth
3	Annual (September–August) response, controlling for drought	$y_{ct} = \alpha_c + \beta_1 \underset{[0,X],\text{annual}}{\text{low\_degree\_days}_{st}} + \beta_2 \underset{(X,+\infty),\text{annual}}{\text{high\_degree\_days}_{st}} + \delta_1 \text{precip}_{st} + \delta_2 \text{precip}^2{}_{st} + \delta_3 \text{age}_{ct} + \delta_4 \text{spei (1, 3, 12 months)}_{st} + \varepsilon_{ct}$	Same as above	Same as model 1, but holding drought levels constant
4	Seasonal (AMJJA) response, controlling for drought	$y_{ct} = \alpha_c + \beta_1 \underset{[0,X],\text{AMJJA}}{\text{low\_degree\_days}_{st}} + \beta_2 \underset{(X,+\infty),\text{AMJJA}}{\text{high\_degree\_days}_{st}} + \delta_1 \text{precip}_{st} + \delta_2 \text{precip}^2{}_{st} + \delta_3 age_{ct} + \delta_4 \text{spei (1, 3, 12 months)}_{st} + \sigma \text{splines (}Sep - \text{March temperature)}_{st} + \varepsilon_{ct}$	Same as above	Same as model 2, but holding drought levels constant
5 a. b. c. d.	(a.c.) annual or (b.d.) AMJJA response, controlling for lagged weather (and drought for c.d.)	$y_{ct} = \alpha_c + \beta_1 \underset{[0,X],\text{annual}}{low\_\text{degree\_days}_{st}} + \beta_2 \underset{(X,+\infty),\text{annual}}{\text{high\_degree\_days}_{st}} + \delta_1 \text{precip}_{st} + \delta_2 \text{precip}^2{}_{st} + \delta_3 age_{ct} + \delta_4 \text{spei (1, 3, 12 months)}_{st} + \gamma_1 \text{splines (}Sep - Aug \text{ temperature)}_{s,t-1} + \gamma_2 \text{precip}_{s,t-1} + \gamma_3 \text{precip}^2{}_{s,t-1} + \gamma_4 \text{spei (1, 3, 12 months)}_{s,t-1} + \varepsilon_{ct}$	Same as above	Same as (a.) model 1, (b.) model 2, (c.) model 3, and (d.) model 4, but holding last year's weather constant
Temperature response curve, by trait				
6 a. b.	Seasonal (AMJJA) response	models (a.) 2 and (b.) 4, estimated for the sample of temperature-sensitive trees	Same as above	Same as model 2, but for temperature-sensitive trees
7	annual (September–August) response	model 1, estimated by isohydric status	Same as above	Same as model 1, but for (a) isohydric trees (b) anisohydric trees
Application				
8	Distributed lag model	$y_{ct} = \alpha_c + \sum_{i=0}^{10} \beta_{1,i} \underset{[0,X],\text{annual}}{low\_\text{degree\_days}_{s,t-i}} + \sum_{i=0}^{10} \beta_{2,i} \underset{(X,+\infty),\text{annual}}{\text{high\_degree\_days}_{s,t-i}} + \sum_{i=0}^{10} \delta_{1,i} \text{precip}_{s,t-i} + \sum_{i=0}^{10} \delta_{2,i} \text{precip}^2{}_{s,t-i} + \delta_3 age_{ct} + \varepsilon_{ct}$	X is taken from model 1 (ecoregion specific)	Impact of low and high degree days, across a 10-year horizon

TABLE 1 (Continued)

Model number	Short description	Equation	Breakpoint identification	Core interpretation
9	Acclimatization to high temperatures	$y_{ct} = \alpha_c + \beta_1 low\_degree\_days_{st}$ $_{[0,X],annual}$ $+ \beta_2 high\_degree\_days_{st}$ $_{(X,+\infty),annual}$ $+ \gamma_{lat,lon} * low\_degree\_days_{st}$ $_{[0,X],annual}$ $+ \eta_{lat,lon} * high\_degree\_days_{st}$ $_{(X,+\infty),annual}$ $+ \beta_3 youthExposure_c * low\_degree\_days_{st}$ $_{[0,X],annual}$ $+ \beta_4 youthExposure_c * high\_degree\_days_{st}$ $_{(X,+\infty),annual}$ $+ \delta_1 precip_{st} + \delta_2 precip^2_{st} + \delta_3 age_{ct} + \varepsilon_{ct}$	X is taken from model 1 (ecoregion specific)	Impact of youth exposure to high degree days on adult growth response to high degree days
10	Adaptation to high temperatures	model 1, estimated by weather grid cell; then β_2, grid cell is regressed against grid-cell level climate	X is taken from model 1 (sample specific e.g., humid ecoregions, Douglas Fir, etc.)	Impact of average incidence of high degree days on growth response to high degree days

spatial correlation in the error term is taken into account when estimating standard errors (see Supplemental Materials and Methods 2.3 in Appendix S1 for more details on the age control and clustering of standard errors). Overall, the following spatial scales are involved: the model is specified at the tree core level, temperature and precipitation vary at a 4 km resolution, SPEI varies at a 0.5° resolution, the estimation of standard errors allows for correlated errors up to a 2° range, and the model is estimated separately for each ecoregion of the United States, to allow for heterogeneity in the temperature response.

The key coefficients of interest are β_1, which represents the impact of an additional degree day below breakpoint X, and β_2, which represents the impact of an additional degree day above breakpoint X. To represent this model graphically, I plot those two coefficients as slopes across a [0–40°C] temperature range. Essentially, it is as if the temperature of a fictitious day was varying between 0°C and 40°C, and the corresponding change in log tree width was plotted against temperature. The temperature curve obtained represents the impact of a given day's temperature, relative to a temperature of 0°C for that day, averaged across all days in the year.

2.4.2 | Spline-based response to temperature

To test whether the growth–temperature relationship emerges as piecewise linear without imposing a restrictive functional form, I estimate a more flexible spline-based model in temperature (Supplemental Materials and Methods 2.4). A similar model has been used to study the temperature response of crops (Schlenker & Roberts, 2009). I do not use this spline model widely, because cross-curve comparisons are difficult and high-order spline curves can behave wildly at the extremes, which prevents precise analysis of the impact of high temperatures (Albouy et al., 2016).

2.5 | Temperature response curve: Variations on the baseline model, by ecoregion

2.5.1 | Seasonal model: Response to spring–summer temperature

The baseline annual model averages the impact of a given temperature exposure across all seasons within a year. This could mask heterogeneity in seasonal temperature responses, in the temperature ranges that overlap across seasons. For instance, the temperature response curve in the mid-temperature range could be driven both by the impact of a warmer winter and by the impact of a warmer spring. At high elevations in dry climates, the former would translate into lower growth, due to thinner snowpack, hence lesser recharge of spring moisture, while the latter would translate into higher growth. Mixing seasonal temperature responses could also impact the temperature response outside

of the range where seasonal temperatures overlap, given the low degrees of freedom of the piecewise linear functional form. To further isolate the impact of temperature, and of high temperatures specifically, a spring–summer temperature response model is estimated (Table 1, model 2). It has the same structure as the baseline annual model, with two differences: all weather variables—degree days and precipitation—are summed over the spring–summer season, defined as the months of April through August (AMJJA); and the model includes controls for September-to-March temperature, in the form of splines in temperature aggregated over that season.

2.5.2 | Annual and seasonal models: Controlling for drought

The baseline and seasonal models capture the impact of temperature changes, inclusive of associated changes in coupled factors. One such factor, drought, is likely to play a dominant role in shaping the temperature response curves, especially in dry ecoregions BSk and Csb, given strong drought sensitivity in the ITRDB data (Williams et al., 2013). In order to understand how much the temperature response curves are driven by temperature-mediated drought conditions, a "drought-free" temperature response is estimated by controlling for drought (Table 1, models 3 and 4). These annual and seasonal models include monthly values of the 1-month, 3-month, and 12-month SPEI, to capture both short-term and medium-term drought conditions, and control for drought flexibly. In the annual model, all months from September of the previous year to August of the current year are included for the 1-month SPEI; the months of November, February, May, and August for the 3-month SPEI; and the month of August for the 12-month SPEI. In the seasonal AMJJA model, all AMJJA months are included for the 1-month SPEI; the months of May, and August for the 3-month SPEI; and the month of August for the 12-month SPEI. Since the x-month SPEI takes into account drought conditions in the previous x months, this avoids excessive correlation across monthly SPEI values, and matches the year or season that is used to construct the temperature and precipitation variables.

2.5.3 | Annual and seasonal models: Controlling for past weather

Weather conditions can be correlated from one year to the next, and weather from the previous year can impact current tree radial growth via impacts on carbon uptake, root and xylem structures, or the timing of dormancy (Begum et al., 2018; Trugman et al., 2021). The baseline temperature response curves could thus partially reflect lagged temperature impacts. To further isolate the impact of current temperature, a lagged version of the annual and seasonal models, with and without drought controls, is estimated (Table 1, models 5 a.–d.). It includes controls for a single lag of all weather variables: splines in temperature, a quadratic in precipitation, and drought variables when applicable.

2.6 | Temperature response curve: Heterogeneity by trait

The previous models focus on heterogeneity in the temperature response across ecoregions. The following two models explore instead heterogeneity in the temperature response across specific tree traits: temperature sensitivity on the one hand, and isohydric status on the other hand.

2.6.1 | Sample restriction: Temperature-sensitive trees

In the ITRDB dataset, many trees primarily respond to drought, but some trees primarily respond to temperature. I call the latter "temperature-sensitive" trees. I identify them using the raw correlation between log ring width and cumulative AMJJA temperature, and the criteria that this correlation be strictly positive (Babst et al., 2013; George, 2014). The spring–summer response of these trees is estimated by fitting the seasonal AMJJA model to this restricted sample (Table 1, model 6). To test the expectation that the temperature response of temperature-sensitive trees reflects mostly direct temperature impacts and not temperature-driven drought impacts, the seasonal AMJJA model that includes drought controls is also estimated for this sample of trees.

2.6.2 | Sample restriction: Isohydric versus anisohydric trees

Isohydric trees tend to close their stomata when soil moisture decreases or VPD increases to avoid transpiring, while anisohydric trees adopt a riskier behavior and keep their stomata open longer under dry conditions (Allen et al., 2010). Temperature response curves can be used to test whether the greater stomatal control of isohydric trees translates into a stronger response to high temperatures, if avoiding the risk of hydraulic failure is costly for growth due to lower carbon uptake. I assign an anisohydric status to all oak and juniper species, and an isohydric status to all pine, spruce, and tulip species (Liu et al., 2019; McDowell et al., 2008; Roman et al., 2015; Zweifel et al., 2009), with the caveat that there is usually a continuum of behaviors on the isohydric–anisohydric spectrum (Klein, 2014; Yi et al., 2017). Despite strong geographic clustering of tree species in the ITRDB dataset, there is some spatial overlap between isohydric and anisohydric tree species in three ecoregions: Csb in the West, Dfb in the North-East and South-West, and Cfa in the South-East (Supplemental Materials and Methods 1.4 in Appendix S1). The baseline annual temperature model is estimated for isohydric and anisohydric trees separately, within each of those ecoregions (Table 1, model 7).

2.7 | Applications of the temperature response curve

When a temperature response curve is estimated, the breakpoint capturing the key non-linearity is not imposed, it is selected in the [1–40°C] range using 10-fold cross-validation. In what follows, I use these flexible temperature response curves, taking their optimal breakpoint as given, but allowing model coefficients to vary, to explore three facets of the impact of high temperatures on growth: I estimate the long-term impact of high temperatures, the extent to which trees acclimatize to high temperatures throughout their lifetime, and the extent to which spatial variation in the temperature response reflects long-term adaptation to high temperatures.

2.8 | Long-term impact of temperature

Trees store resources, in particular carbon, such that the carbon that they use to grow a new ring can come from carbon acquired in previous years (Castagneri et al., 2018). This means that past weather can have a strong impact on current growth. In addition, trees are long lived, and can react to a harmful weather event over several years, possibly compensating for growth failures by additional growth in later years (DeSoto et al., 2020). I document legacy effects of temperature by estimating a distributed lag model, which includes 10 years of lags of low degree days and high degree days (Table 1, model 8). This timeline should be sufficient to capture legacy effects, based on evidence from drought and tree growth (Anderegg et al., 2015; DeSoto et al., 2020). In this model, the optimal breakpoint used to split temperature into low and high degree days comes from the baseline annual model (model 1) and is ecoregion specific.

2.9 | Acclimatization analysis

Temperature response curves can be used to test whether individual trees can adapt to high temperatures within their lifetime. Specifically, I test whether the temperature response of a mature tree varies, as a function of the weather sequence experienced during their youth. I formulate two competing hypotheses (Figure 3). The first holds that trees that experience high temperatures more frequently during their youth, learn to buffer temperature-induced growth fluctuations. This allows them to survive high-temperature events without sacrificing much growth, which can be interpreted as a sign of higher fitness (DeSoto et al., 2020). This type of priming has been documented in the short term: experiencing high heat triggers tolerance mechanisms, which can be more easily triggered in future—potentially more damaging—high heat events, on a timescale of hours to months (Nievola et al., 2017). Here I posit that priming could also work on a timescale of years to decades. The second hypothesis holds that trees that experience high temperatures more frequently during their youth, accumulate damage and lose the ability to respond optimally to high-temperature events. This implies greater growth decreases under high-temperature events during the rest of their life. A mechanism could be long-term damage to the tree's root system.

To test these hypotheses, I use the ecoregion-level temperature breakpoint as a fixed breakpoint, and allow the impact of temperatures above that breakpoint ("high temperatures") to vary with the intensity of early life exposure to high temperatures (Table 1, model 9). In that setting, hypothesis 1 corresponds to a milder impact of high temperatures, following more intense exposure to high temperatures during youth; hypothesis 2 corresponds to a stronger impact of high temperatures, following more intense exposure to high temperatures during youth. The "priming" youth period for trees is

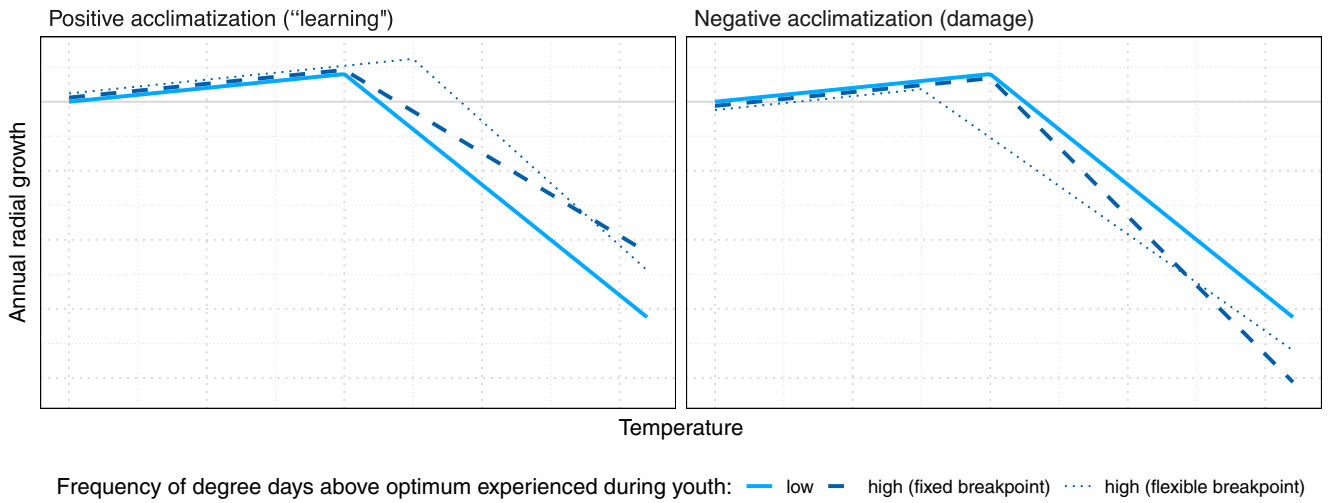

FIGURE 3 Acclimatization hypotheses. The solid curve is the schematic temperature response curve of an average tree. The other curves are the schematic departures from this average response, for a tree that has experienced relatively more degree days above the regional optimum. The dashed curve represents departure when the non-linearity breakpoint is fixed; the dotted curve represents departure when the non-linearity breakpoint is flexible; it illustrates how a change in the "true" breakpoint can still manifest as a dashed curve if a fixed-breakpoint model is estimated. Left: Acclimatization as "learning." Right: Acclimatization as accumulated damage. [Colour figure can be viewed at wileyonlinelibrary.com]

defined as the first decade of their life (Supplemental Materials and Methods 2.5 in Appendix S1), while the rest of their life is used to estimate their long-term response to temperature. The main measure of early exposure to high temperatures is the annual number of high degree days experienced by a tree, averaged over its youth. Alternative measures of exposure use maximum or 90th percentile functions to aggregate annual exposure to high degree days over a tree's youth. The model equation is as follows:

$$y_{ct} = \alpha_c + \beta_1 \underset{[0,X],\text{annual}}{\text{low\_degree\_days}_{st}} + \beta_2 \underset{(X,+\infty),\text{annual}}{\text{high\_degree\_days}_{st}} + \gamma_{\text{lat,lon}} * \underset{(X,+\infty),\text{annual}}{\text{low\_degree\_days}_{st}} + \beta_3 \text{youthExposure}_c * \underset{(X,+\infty),\text{annual}}{\text{low\_degree\_days}_{st}} + \eta_{\text{lat,lon}} * \underset{(X,+\infty),\text{annual}}{\text{high\_degree\_days}_{st}} + \beta_4 \text{youthExposure}_c * \underset{(X,+\infty),\text{annual}}{\text{high\_degree\_days}_{st}} + \delta_1 \text{precip}_{st} + \delta_2 \text{precip}^2{}_{st} + \delta_3 \text{age}_{ct} + \varepsilon_{ct}$$

$$\text{where,} \quad \text{youthExposure}_c = \frac{1}{10} \sum_{\tau=\text{year of birth}}^{\text{year at age 10}} \underset{(X,+\infty),\text{annual}}{\text{high\_degree\_days}_{s\tau}}$$

The youth exposure variable varies by tree core c and not by weather grid cell s because it is a weather aggregate over a tree-specific period, which depends on when the tree was born. Threshold X is ecoregion specific, and determined using the baseline annual model (model 1). The high degree day variable is interacted with location fixed effects $\eta_{\text{lat,lon}}$, that is, location dummy variables, where lat and lon are rounded to the closest degree, so that the exposure interaction term captures differences in temperature impacts between trees that live close by, but have experienced different weather histories early in life, due to differences in the timing of their birth. Additional controls are similar to the baseline annual model. The conflicting hypotheses tested are $\beta_4 > 0$ (acclimatization as "learning") versus $\beta_4 < 0$ (acclimatization as accumulated damage). The model includes a similar interaction term for the low degree day variable, with the expectation that the interaction coefficient β_3 is not significantly different from zero.

As an alternative to the youth–adulthood timeline, I test for acclimatization on a decadal timescale, where the temperature response of a tree in a given decade, can vary as a function of the weather experienced during the previous decade. This allows for continual acclimatization to high temperatures throughout a tree's life. The structure of the model is similar to that described above: high-temperature exposure during a given decade, is interacted with high-temperature exposure during the previous decade along with location fixed effects.

2.9.1 | Adaptation analysis

Temperature response curves can also be used to document the result of long-term adaptation to high temperatures across tree generations, by comparing responses across climatic gradients. I first pool all humid ecoregions (Dfa, Dfb, Dfc, and Cfa), and estimate the baseline annual model (model 1) to find the optimal breakpoint X for this pooled region. I then estimate the baseline annual model again, with breakpoint X fixed, across a spatial grid with 1° resolution spanning all humid ecoregions. This yields grid cell specific estimates of model coefficients, including β_2, which captures the local impact of high temperatures. I regress these coefficients against the average incidence of high temperatures in each grid cell, to test whether tree growth suffers less from high temperatures, in locations where those are more frequent (Table 1, model 10). Alternatively, adaptation is documented across the Cfa ecoregion, and across pooled locations for each of the most widely distributed species (Douglas Fir, Ponderosa Pine and White Oak).

2.10 | Model estimation

The analyses were conducted in R software using the "lfe" package (Gaure, 2021; R Core Team, 2021), with the exception of the search for the optimal breakpoint, which was conducted using the "reghdfe" package in Stata software version 16 (StataCorp, 2019). This package minimizes runtime when estimating a linear regression with many levels of econometrics-style fixed effects. This time gain is key for the breakpoint search, which requires fitting 400 regressions per ecoregion (40 possible breakpoints, each assessed using 10-fold cross-validation), and where each regression includes as many levels of fixed effects (i.e. dummy variables) as there are tree cores in an ecoregion.

The models described in Table 1 each answer a different question around the impact of temperature on radial tree growth. As such, the focus is on the coefficients associated with the temperature variables, and how their value and interpretation vary with different modeling assumptions (i.e., sets of predictors), and the focus is not on the relative predictive performance of the different models.

3 | RESULTS

3.1 | Temperature response curve: Baseline model (by ecoregion)

3.1.1 | Piecewise linear response to temperature

The annual temperature response of tree ring width varies across ecoregions and often displays non-linearity (model 1, Figure 4, "annual" curve, Tables S1–S6). In ecoregions Dfa, Cfa, and Csb, temperature increases have a relatively neutral or slightly positive impact on tree growth up to a temperature threshold of 17°C, 26°C, and 7°C, respectively, beyond which tree growth decreases sharply with further temperature increases. The temperature threshold is higher in humid ecoregions Dfa and Cfa than in dry ecoregion Csb. In ecoregions Dfb and BSk, the pattern is similar but with a much lower temperature threshold of 1°C. In ecoregion Dfc, the impact of temperature increases is consistently negative, with a more negative impact starting at 19°C. The negative impact of high temperatures,

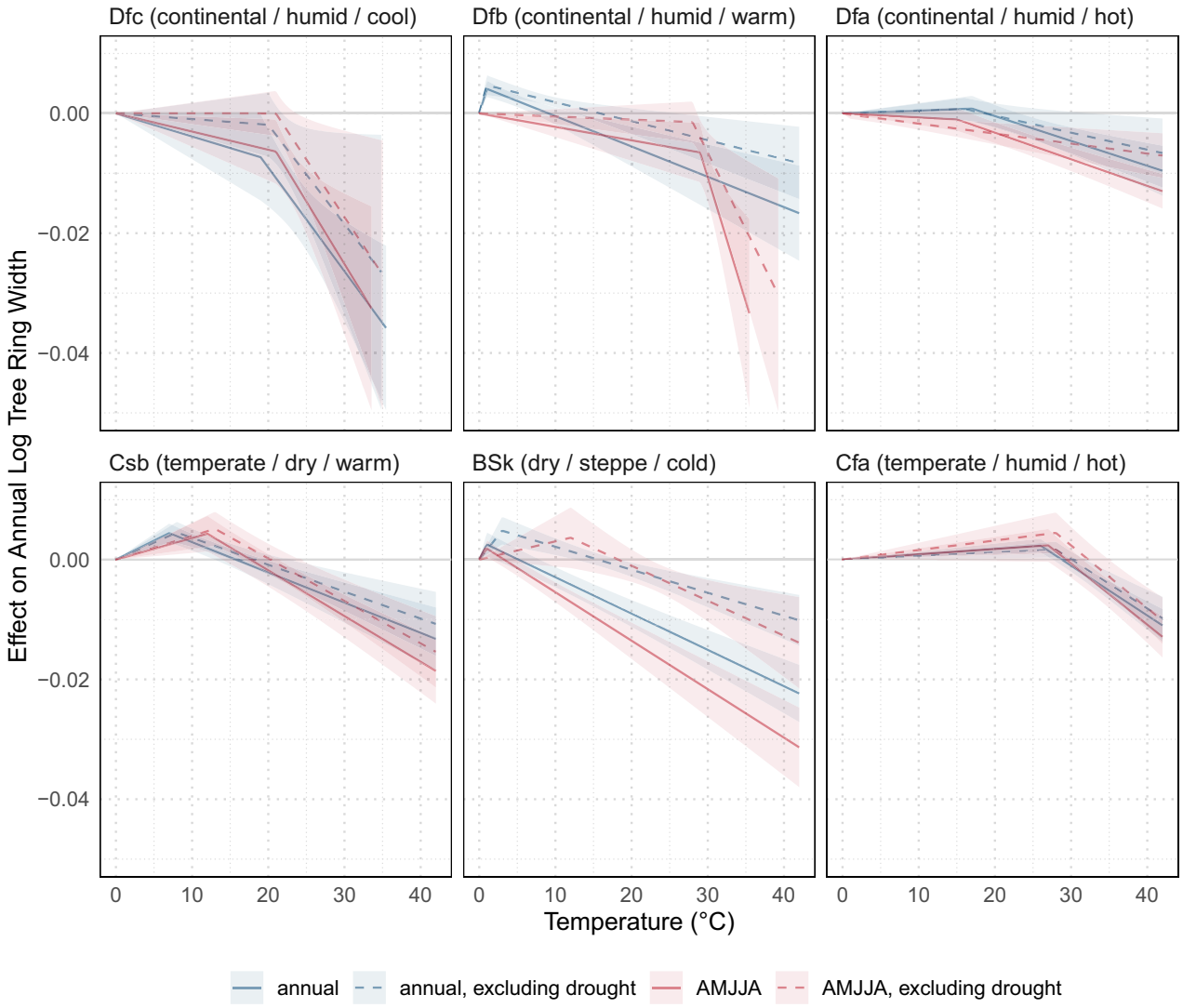

FIGURE 4 Piecewise linear relationship between annual log ring width and temperature (models 1–4). The optimal breakpoint is identified in the 1–40°C range, using 10-fold cross-validation across years. All models include tree core fixed effects, a quadratic in total annual precipitation, a linear control in age, and standard errors clustered at the 2° grid cell level. The "annual" models aggregate low and high degree days across the year (from the previous September to the current August), while the "AMJJA" models aggregate low and high degree days across the spring and summer seasons, and control for September–March temperature. In addition, the models "excluding drought" control for monthly values of the 1-month, 3-month, and 12-month SPEI. The 95% confidence interval is added as a lighter area around the curve. Each graph corresponds to a different ecoregion of the United States. [Colour figure can be viewed at wileyonlinelibrary.com]

captured by the upper slope value, is always statistically significant but varies in magnitude across ecoregions. An additional 30 "high" degree days during the year, which is equivalent to adding 1°C to each day during a month where temperatures are consistently above the optimal threshold, has the following impact: it decreases annual tree ring width by 5.2% on average in Dfc, 1.5% in Dfb and Csb, 1.2% in Dfa, 1.8% in BSk, and 2.5% in Cfa. Confidence intervals are particularly wide in continental ecoregions (Dfa, Dfb, and Dfc). This could be because of lower variability in temperature in these ecoregions. In particular, temperature varies at the scale of PRISM grid cells, and tree ring sites in Dfa and Dfc overlap with 50 and 70 PRISM grid cells respectively, compared to more than 200 grid cells for the other ecoregions. The more flexible spline-based curves suggest that a piecewise linear function is a relevant approximation of the growth-temperature relationship (Supplemental Materials and Methods 3.2 in Appendix S1).

3.2 | Temperature response curve: Variations on the baseline model (by ecoregion)

3.2.1 | Seasonal model: Response to spring–summer temperature

Spring–summer AMJJA temperature response curves are overall similar to annual temperature response curves, with the exception of ecoregion Dfb (model 2, Figure 4, "AMJJA" curve, Tables S1–S6). The optimal breakpoint increases in all ecoregions, except for BSk

where it does not change, and Dfa where it decreases. The negative impact of high temperatures becomes particularly stronger in dry ecoregions Csb and BSk: it now respectively amounts to an average decrease of 2.3% and 2.8% per 30 additional "high" degree days, compared to a 1.5% and 1.8% decrease for the annual response.

3.2.2 | Annual and seasonal models: Controlling for drought

Controlling for drought using the 1-month, 3-month, and 12-month SPEI changes the annual temperature response curve in many ecoregions (model 3, Figure 4, "annual, excluding drought" curve, Tables S1–S6). In Dfc and BSk, the impact of low degree days increases; in Dfb, Dfa, Csb, and BSk the impact of high degree days increases; and in Cfa there is little change. This suggests that in many ecoregions, negative drought-mediated temperature impacts account for part of the response of ring width to temperature. The influence of drought is especially visible in dry ecoregion BSk where the overall change in the temperature response curve with the inclusion of drought is the most significant. Controlling for drought changes the AMJJA temperature response curves in a similar pattern (model 4, Figure 4, "AMJJA, excluding drought" curve, Tables S1–S6). The increase in the optimal breakpoint in BSk and Cfa is more pronounced. When controlling for drought, the negative impact of AMJJA temperature increases starts at 21°C in Dfc, 28°C in Dfb, 13°C in Csb, 12°C in BSk, 28°C in Cfa, while in Dfa, the impact of temperature increases is consistently negative, with a more negative impact starting at 1°C. Adding 30 "high" degree days to the spring–summer season, holding drought constant, decreases annual tree ring width by 5.6% on average in Dfc, 7.2% in Dfb, 0.5% in Dfa, 2.1% in Csb, 1.7% in BSk, and 3.1% in Cfa.

3.2.3 | Annual and seasonal models: Controlling for past weather

Controlling for a 1-year lag in temperature, precipitation, and drought when applicable, yields very similar temperature response curves (Figure S7). These models include many predictors, which might explain why confidence intervals widen in some ecoregions, especially the three continental ones. Breakpoint identification is challenging in this context since it is based on differences in predictive performance, which might be less evident when estimation is less precise. In the other ecoregions, the optimal breakpoints tend to increase, more so in dry Csb and BSk than in humid Cfa. When controlling for drought and past weather, the negative impact of AMJJA temperature increases starts at 15°C in Csb, 14°C in BSk, and 19°C in Cfa. Adding 30 "high" degree days to the spring–summer season, holding drought and past weather constant, decreases annual tree ring width by 2.3% on average in Csb, 1.6% in BSk, and 3.6% in Cfa.

Overall, variations around the baseline temperature response (models 1–5) suggest that a non-linear representation of the impact of temperature on growth is particularly suited to the temperate ecoregions, Cfa and Csb, and to some extent to dry ecoregion BSk. In continental ecoregions, identification of the best temperature breakpoint is more sensitive to model specification, and confidence intervals are consistently wide. Imposing a fixed breakpoint, based on the underlying climate in each ecoregion, confirms this pattern (Figure S8).

3.3 | Temperature response curve: Baseline model (heterogeneity by trait)

3.3.1 | Sample restriction: Temperature-sensitive trees

The spring–summer AMJJA temperature response curve of temperature-sensitive trees displays strong non-linearity (Figure 5). Increases in temperature have a strong positive impact on tree growth until the optimal level of 32°C, beyond which the impact turns negative. In practice, an additional 30 degree days above 32°C translates into a 14% decrease in tree ring width on average. Relative to ecoregion-level curves, this temperature response is closer to the leaf-level response of net photosynthesis to temperature, which reflects direct temperature effects on the rates of carbon exchange processes. In addition, it is not impacted by the exclusion of drought

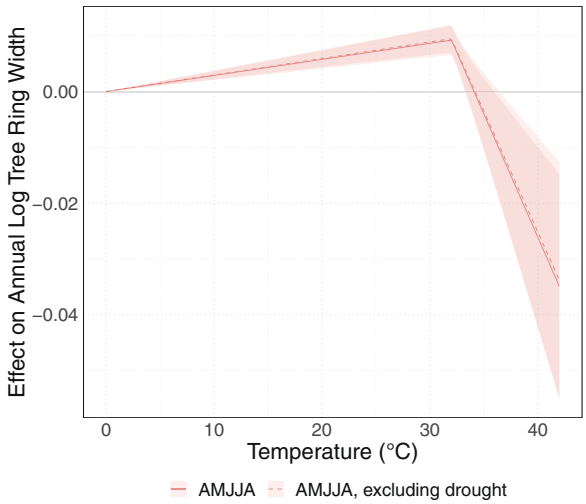

FIGURE 5 Piecewise linear relationship between annual log ring width and AMJJA temperature for temperature-sensitive trees (models 6 a. and b.). The optimal breakpoint is identified in the 1–40°C range, using 10-fold cross-validation across years. The models used are the seasonal (AMJJA) models 2 and 4, which respectively include and exclude drought effects. They include tree fixed effects, a quadratic in total annual precipitation, a linear control in age, and standard errors clustered at the 2° grid cell level. The model "excluding drought" also includes a 1-year lag in all monthly SPEI variables. The 95% confidence interval is added as a lighter area around the curve. The sample is restricted to temperature-sensitive trees.-[Colour figure can be viewed at wileyonlinelibrary.com]

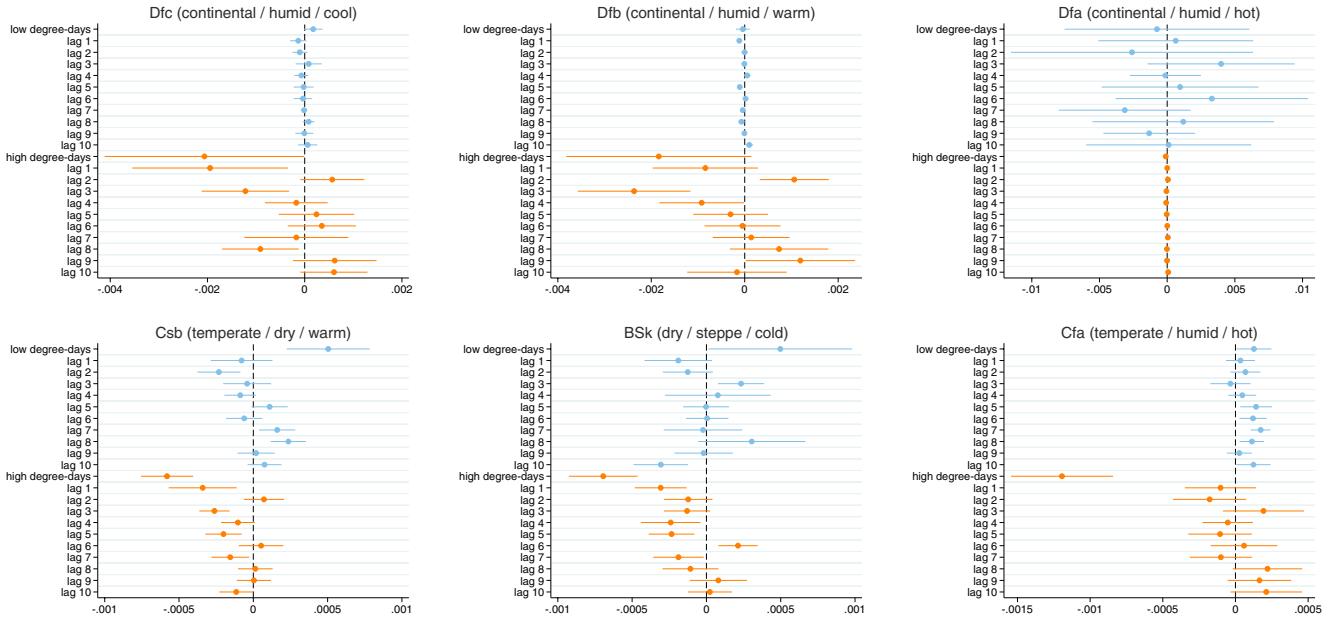

FIGURE 6 AMJJA temperature coefficients from a distributed lag model (AMJJA-drought version of model 8). The outcome is annual log ring width, and the model includes 10 lags of AMJJA low degree days and high degree days. The temperature threshold used to distinguish low and high degree days is the optimal breakpoint identified in AMJJA-drought model 4 for each ecoregion. The model also includes tree fixed effects, a quadratic in total annual precipitation along with 10 lags, spline-based controls for September–March temperature, monthly values of the 1-month, 3-month, and 12-month SPEI, a linear control in age, and standard errors clustered at the 2° grid cell level. Each graph corresponds to a different ecoregion of the United States. [Colour figure can be viewed at wileyonlinelibrary.com]

effects, consistent with temperature being the limiting growth factor for this sample of trees.

3.3.2 | Sample restriction: Isohydric versus anisohydric trees

Across the three ecoregions where isohydric and anisohydric species overlap, isohydric trees seem to suffer more from high temperatures (Figure S10, model 7). The negative impact of "high" temperatures is stronger for isohydric species, which suggests that a more cautious stomatal adjustment has an immediate cost in terms of radial growth. If the riskier strategy of anisohydric trees is associated with tolerance of a greater range of temperatures, it could have translated into a higher optimal breakpoint. This is not consistently the case across the different ecoregions, although breakpoint identification is not necessarily precise.

3.4 | Applications of the temperature response curve

3.4.1 | Long-term impact of temperature

The cumulative growth impact of high temperatures over 10 years is negative in all ecoregions, whether it is the impact of annual temperatures (model 8, Figure S11) or the impact of AMJJA temperatures after controlling for drought (AMJJA-drought version of model 8, Figure 6). The magnitude of the contemporaneous impact of high temperatures is often greater than the magnitude of lagged impacts. There is little evidence of rebound growth and some evidence of negative lagged impacts persisting over time. These patterns become more evident when focusing on ecoregions where the temperature response curve is more reliable—that is to say with a more stable optimal breakpoint, and tighter confidence intervals: specifically the annual and AMJJA-drought responses in Cfa and Csb, and AMJJA-drought response in BSk. Ecoregion Cfa is notable for its clear absence of lagged impacts, compared to Csb and BSk where high temperatures have a persistent negative impact over approximately 5 years. For temperature-sensitive trees, the same clear absence of lagged impacts and prominence of the contemporaneous impact of high temperatures, are observed (Figure S12).

3.5 | Acclimatization to high temperatures

In the acclimatization model (Table 1, model 9), the interaction coefficient between high degree days and early exposure to high temperatures, represents how much the exposure of trees to high temperatures during youth, shapes their response to high temperature later on, relative to neighboring trees. A positive value indicates acclimatization as "learning," and a negative value indicates acclimatization as accumulated damage. This interaction coefficient is very small across ecoregions, for both the annual model (Figure S13, Tables S7–S12) and the AMJJA-drought model (Tables S13–S18). It is only significantly different from zero in Dfa and Csb for the annual

model, where it is positive and small. This suggests that there is no acclimatization to high temperatures at this timescale. Interacting high degree days with 1° location fixed effects aims to compare trees with different early exposures in the same location, which likely absorbs a lot of variation in early exposure. Interacting high degree days instead with a measure of the average climate at each location, to compare trees with different early exposures in similar climatic environments but possibly different locations, does not change the results.

Among temperature-sensitive trees, there is some evidence of acclimatization as accumulated damage (Figure 7, Table S19). Based on the model that defines early exposure as the average frequency of high temperatures during youth (`avg ddayHigh` column), the magnitude of acclimatization is as follows: for a one standard deviation increase in early exposure—which corresponds for example to an extra 8.6 degree days above 32°C experienced annually during the first 10 years of life—the harmful impact of high temperatures later in life increases by 12% or 0.08 percentage points.

There is little evidence of acclimatization on a decadal timescale (Tables S20 and S21). In Cfa and Dfc, trees tend to suffer more from high temperatures following a decade with higher incidence of high temperatures. The opposite holds in Dfa for the annual response. In both cases, magnitudes are as small as for the youth-to-adulthood acclimatization timescale.

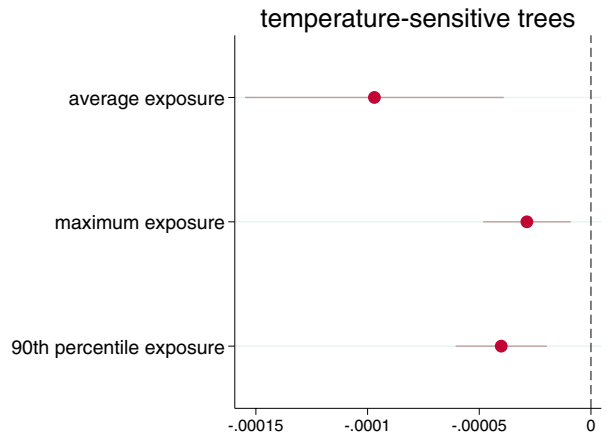

FIGURE 7 Main coefficient estimates from an AMJJA version of acclimatization model 9, restricted to the sample of temperature-sensitive trees. Each coefficient represents the change in the impact of AMJJA degree days above the optimal breakpoint, as early exposure to AMJJA high degree days increases. The temperature threshold used to distinguish low and high degree days is the optimal breakpoint identified in AMJJA model 6 a. for temperature-sensitive trees. The model also includes tree fixed effects, 1° location fixed effects interacted with low and high degree days, a quadratic in total annual precipitation, a linear control in age, and standard errors clustered at the 2° grid cell level. Three variations of the model are estimated, which correspond to three different measures of early tree exposure to high temperatures: Starting from total annual high degree days experienced by a tree, (1) "average exposure" is the average value of annual high degree days over the years of the tree's youth; (2) "maximum exposure" is the maximum value over the tree's youth; and (3) "90th percentile exposure" is the 90th percentile over the tree's youth. [Colour figure can be viewed at wileyonlinelibrary.com]

3.6 | Adaptation to high temperatures

When all humid ecoregions are pooled, the optimal temperature breakpoint for capturing non-linear impacts is at 22°C. Spatial variation in the impact of annual high degree days above 22°C across 1° grid cell in that region provides some evidence of long-term adaptation to those temperatures (Figure 8a,b). High degree days above 22°C have a more negative impact in the West, where those temperatures are relatively less frequent, than in the East. A similar pattern exists along a latitudinal gradient in the East, although it is less apparent. On average, a one standard deviation increase in the average incidence of high temperatures, corresponds to lower damage from those temperatures by 40%, as the impact of an additional 30 high degree days changes from −3% to −1.8% (Figure 9a). This relationship is strongly driven by the lower tolerance to high temperature in locations where high temperatures are very rare, even when focusing on grid cells where the impact of high temperatures is negative and statistically significant (Figure 9b).

There is mixed evidence of adaptation to high temperatures across other samples. For Douglas Fir trees and Ponderosa Pine trees, which tend to occur in dry areas, I use the AMJJA response to temperature, after controlling for drought. For temperate ecoregion Cfa and for White Oak trees, which overlap with both temperate and continental areas, I use the annual response to temperature. There is some adaptation among Douglas Firs to temperatures above 26°C (Figures S17–S19), among Ponderosa Pines to temperatures above 14°C (Figures S20 and S21), and weaker adaptation in Cfa to temperatures above 26°C (Figures S15 and S16), and among White Oaks to temperatures above 14°C (Figures S22 and S23). On average, a one standard deviation increase in the average incidence of high temperatures, corresponds to lower damage from those temperatures by 803% (45% after excluding outliers), 106%, 11% and 14% in each of those respective samples.

4 | DISCUSSION

By combining a hundred years of tree ring data spanning the contiguous United States, with a degree day-based aggregation of temperature, I estimate real-world temperature response curves for tree radial growth across a climatic gradient. I find that many ecoregions are characterized by a non-linear response to temperature, where increases in temperature are neutral or slightly beneficial to growth up to a point, beyond which increases in temperature are harmful to growth. Drought and seasonality influence the shape of this response, in the driest ecoregions particularly, and the non-linearity becomes even more evident when drought-mediated impacts are excluded. This study provides insights into the sub-lethal impacts of high temperatures, into variations in temperature sensitivity across

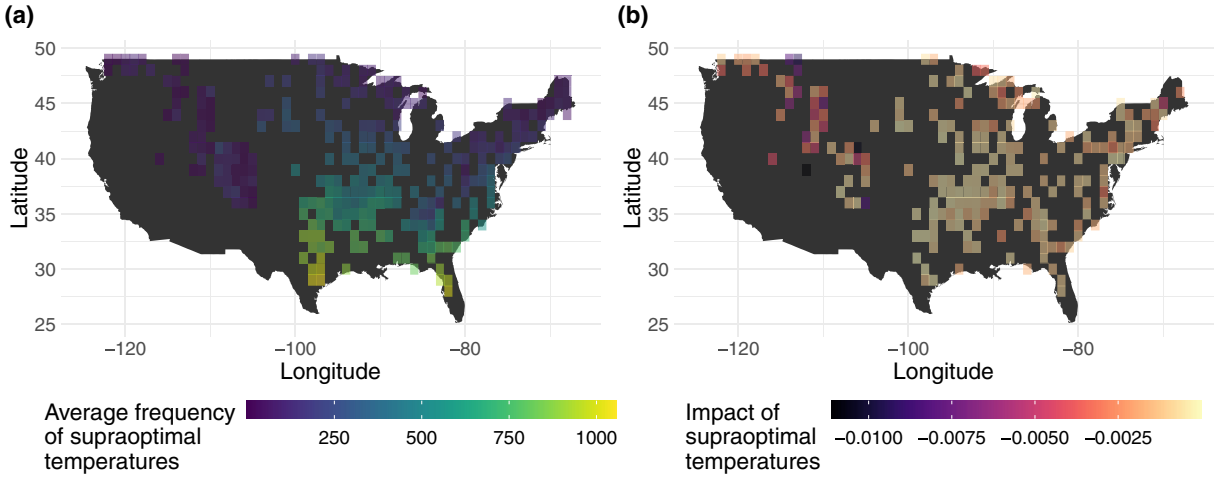

FIGURE 8 Adaptation maps. Frequency and impact of degree days above 22°C in humid ecoregions (selected grid cells). (a) Average number of annual degree days above 22°C, by 1° grid cell. (b) Impact on annual tree growth of an additional degree day above 22°C, in humid ecoregions. The choice of 22°C as a key breakpoint is based on estimating baseline annual model 1 across the pooled sample of humid ecoregions. This fixed-breakpoint model is then run separately on each 1° grid cell within that region. Only negative and statistically significant coefficients are displayed, for graphical clarity (full map in Figure S14). [Colour figure can be viewed at wileyonlinelibrary.com]

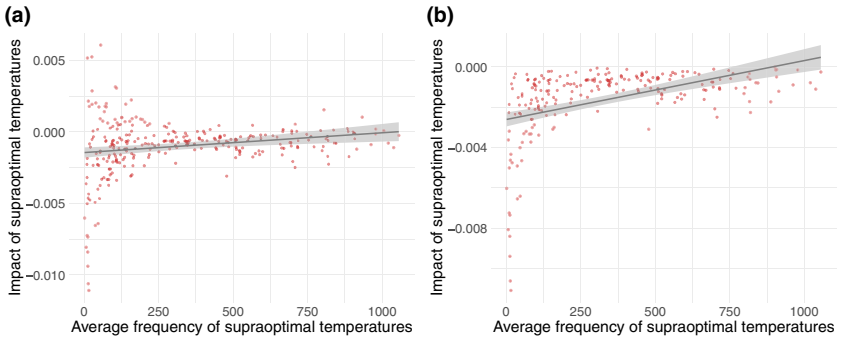

FIGURE 9 Adaptation scatterplot. Impact of degree days above 22°C as a function of their frequency, in humid ecoregions. The units of analysis are 1° grid cells. (a) All grid cells. (b) Grid cells where the impact of degree days above 22°C is negative and statistically significant. [Colour figure can be viewed at wileyonlinelibrary.com]

climate and traits, and into the capacity of trees to recover, acclimatize, and adapt to sub-lethal high temperatures.

The piecewise linear function of seasonal degree days, with flexible breakpoint identification, is particularly suited to capturing the non-linear impacts of temperature in two settings: temperate ecoregions Cfa and Csb, where negative impacts of spring and summer temperature increases start around 27–29°C in humid Cfa and 12–15°C in dry Csb; and dry ecoregion BSk, when drought impacts are controlled for (the non-linearity breakpoint is at 12–14°C in that context). These are relatively low, sub-lethal, levels of temperature. The overall curves imply a negative impact of temperature on growth on average, which is consistent with previous work. Large-scale studies that document the response of tree growth to temperature, find negative correlations between tree ring width and monthly maximum temperature in many spring–summer months across much of North America (Charney et al., 2016; Heilman et al., 2022; Klesse et al., 2020; Restaino et al., 2016), and others find negative correlations between tree ring width and monthly or growing season mean temperature in Europe (Babst et al., 2013, 2019). In contrast, I find that for temperature-sensitive trees, temperature increases have a strong positive impact on growth up to 32°C, which is consistent with the positive correlations between growth and monthly temperature documented in corresponding locations (Charney et al., 2016). An important contribution of my work is to propose a refined perspective on temperature sensitivity: monthly averages and maxima in temperature are likely correlated with high degree days to some extent, but less responsive to complex shifts in the temperature distribution, which could lead to the underestimation of the temperature sensitivity of trees. The use of an aggregate model and econometric techniques to factor out the influence of observed (e.g., precipitation) and non-observed (e.g., soil type) factors from the temperature impact estimate (Klesse et al., 2020), prevents direct comparison with studies reporting individual correlations between growth and different weather variables (Restaino et al., 2016). Those tools also provide insightful confidence intervals around focal impact estimates.

The non-linear temperature breakpoints are lower than expected, based on the thermal performance curves of photosynthesis (Dreyer et al., 2001; Kattge & Knorr, 2007; Lloyd & Farquhar, 2008; Medlyn et al., 2002) and respiration (Atkin & Tjoelker, 2003; Patterson et al., 2018), which together imply that leaf-level net photosynthesis peaks around 25–35°C in temperate regions (Kattge &

Knorr, 2007; Lloyd & Farquhar, 2008; Medlyn et al., 2002; Waring & Running, 2010). This could be explained by different factors. First, my temperature response curves reflect both direct temperature impacts on enzyme kinetics (Parent et al., 2010) and indirect water-stress impacts on growth via changes in vapor pressure deficit (Lloyd & Farquhar, 2008), and soil moisture (Ma et al., 2017). Ecosystem-level temperature optima for gross primary productivity in the United States, which also reflect direct and indirect impacts, are closer in range to my breakpoint estimates (Huang et al., 2019), and the response of temperature-sensitive species is more aligned with experimental carbon exchange responses that single out direct impacts. The non-linear temperature breakpoints are still low in dry ecoregions when controlling for drought using multi-scale SPEI. However, drought is a multi-faceted phenomenon, and I do not control directly for soil moisture, so those temperature response curves could be impacted by leftover variation in temperature-mediated drought conditions. Second, tree radial growth is influenced by many complex temperature-sensitive processes beyond carbon assimilation, such as the timing of cambial reactivation in temperate regions (Begum et al., 2018), or turgor-driven cell growth, which responds to water stress, influences carbon allocation within the tree (Fatichi et al., 2014), and can become a limiting factor to growth (Peters et al., 2021). Third, temperature increases could impact growth via other pathways, like beneficial increases in nutrient availability (Melillo et al., 2002), although likely to occur over long timescales, and a higher probability of insect and pathogen outbreaks (Hicke et al., 2012; Trugman et al., 2021).

The flexibility of an aggregate model, and the large spatiotemporal variation provided by ITRDB tree ring data, provide opportunities for looking beyond temperature sensitivities. The finding that high temperatures undermine growth over a 5-year horizon in dry BSk and temperate-dry Csb is consistent in timing and magnitude with observed 2–4-year legacy effects of drought (Anderegg et al., 2015). I also find that the concurrent impact of temperature is the strongest, which is what George (2014) observes for the impact of average summer temperature, although maximum temperature in the previous summer displays the strongest correlation with Douglas-fir growth (Klesse et al., 2020), particularly at higher latitudes (Restaino et al., 2016), and the pattern is mixed for drought and boreal trees (Itter et al., 2019). I do not find much evidence of acclimatization on youth-to-adulthood or decadal timescales, except for negative impacts of early exposure on later sensitivity for temperature-sensitive trees. It could be that trees with a higher temperature optimum, operate closer to the end of their safe range (O'sullivan et al., 2017), and that structural defects accumulate under repeated temperature stress, similar to drought (Trugman et al., 2021). Longer term adaptation is visible though not clear-cut, including across humid ecoregions and among two conifer species. Similar spatial variation has been documented for the sensitivity of Douglas Fir to average maximum AMJJA temperature (Restaino et al., 2016).

Non-linear temperature response curves hold a lot of promise for shedding light on the harmful impact of high temperatures, and for projecting tree growth under expected shifts in the temperature distribution. For example, they could be used to investigate the divergence problem at northern latitudes, where decreased sensitivity of tree growth to average temperature has been observed, and could be due to recent shifts in the temperature distribution, combined with a non-linear response of tree growth to temperature (D'Arrigo et al., 2008). Similarly, they could be used to test whether predicted shifts from temperature-limited toward water-limited forest growth could emerge from non-linear responses to temperature and recent shifts in temperature (Babst et al., 2019). The main limitation of this study is that spatial clustering of ITRDB tree ring data limits variation in temperature, which tends to increase standard errors and complicate the identification of the optimal breakpoint. Combined with tree selection in that dataset, this hinders the analysis of heterogeneous responses across species, elevation, and other characteristics. Applying similar models to representative tree ring data from forest inventories could fill some of those gaps and be a crucial step toward characterizing forest-level sensitivity to temperature (DeRose et al., 2017; Evans et al., 2022; Girardin et al., 2021).

ACKNOWLEDGMENTS

I thank Wolfram Schlenker for the initial inspiration behind this work, when he hired me as a research assistant to link tree growth flexibly to weather, and for access to his PRISM-based weather dataset; three anonymous reviewers for their constructive reviews and detailed guidance; Ruth Defries, Kevin Griffin, Claire Kremen, Duncan Menge, Wolfram Schlenker, Naomi Schwartz, Jeffrey Shrader, and all of their laboratory members for constructive and detailed feedback on this project; Brendan Buckley and Edward Cook for invaluable information and advice on the nature and use of tree ring data; Mathias Lécuyer and Rassim Khelifa for their comments on draft versions of the manuscript.

DATA AVAILABILITY STATEMENT

The data that support the findings of this study are available from the dryad repository https://doi.org/10.5061/dryad.v9s4mw6zq. The scripts can be made accessible from the corresponding author upon reasonable request.

ORCID


Joséphine Gantois https://orcid.org/0000-0002-8542-1263

REFERENCES

Albouy, D., Graf, W., Kellogg, R., & Wolff, H. (2016). Climate amenities, climate change, and american quality of life. *Journal of the Association of Environmental and Resource Economists*, *3*(1), 205–246.

Allen, C. D., Breshears, D. D., & McDowell, N. G. (2015). On underestimation of global vulnerability to tree mortality and forest die-off from hotter drought in the anthropocene. *Ecosphere*, *6*(8), 1–55.

Allen, C. D., Macalady, A. K., Chenchouni, H., Bachelet, D., McDowell, N., Vennetier, M., Kitzberger, T., Rigling, A., Breshears, D. D., Hogg,

E. T., Gonzalez, P., Fensham, R., Zhang, Z., Castro, J., Demidova, N., Lim, J.-H., Allard, G., Running, S. W., Semerci, A., & Cobb, N. (2010). A global overview of drought and heat-induced tree mortality reveals emerging climate change risks for forests. *Forest Ecology and Management*, *259*(4), 660–684.

Anderegg, W. R. L., Schwalm, C., Biondi, F., Camarero, J. J., Koch, G., Litvak, M., Ogle, K., Shaw, J. D., Shevliakova, E., Williams, A. P., Wolfe, A., Ziaco, E., & Pacala, S. (2015). Pervasive drought legacies in forest ecosystems and their implications for carbon cycle models. *Science*, *349*(6247), 528–532.

Atkin, O. K., & Tjoelker, M. G. (2003). Thermal acclimation and the dynamic response of plant respiration to temperature. *Trends in Plant Science*, *8*(7), 343–351.

Babst, F., Bouriaud, O., Poulter, B., Trouet, V., Girardin, M. P., & Frank, D. C. (2019). Twentieth century redistribution in climatic drivers of global tree growth. *Science Advances*, *5*(1), eaat4313.

Babst, F., Poulter, B., Trouet, V., Tan, K., Neuwirth, B., Wilson, R., Carrer, M., Grabner, M., Tegel, W., Levanic, T., Panayotov, M., Urbinati, C., Bouriaud, O., Ciais, P., & Frank, D. (2013). Site-and species-specific responses of forest growth to climate across the european continent. *Global Ecology and Biogeography*, *22*(6), 706–717.

Beguería, S., Vicente-Serrano, S. M., Reig, F., & Latorre, B. (2014). Standardized precipitation evapotranspiration index (spei) revisited: Parameter fitting, evapotranspiration models, tools, datasets and drought monitoring. *International Journal of Climatology*, *34*(10), 3001–3023.

Begum, S., Kudo, K., Rahman, M. H., Nakaba, S., Yamagishi, Y., Nabeshima, E., Nugroho, W. D., Oribe, Y., Kitin, P., Jin, H.-O., & Funada, R. (2018). Climate change and the regulation of wood formation in trees by temperature. *Trees*, *32*(1), 3–15.

Bhuyan, U., Zang, C., & Menzel, A. (2017). Different responses of multispecies tree ring growth to various drought indices across europe. *Dendrochronologia*, *44*, 1–8.

Bréda, N., Huc, R., Granier, A., & Dreyer, E. (2006). Temperate forest trees and stands under severe drought: A review of ecophysiological responses, adaptation processes and long-term consequences. *Annals of Forest Science*, *63*(6), 625–644.

Breshears, D. D., Fontaine, J. B., Ruthrof, K. X., Field, J. P., Feng, X., Burger, J. R., Law, D. J., Kala, J., & Hardy, G. E. S. J. (2021). Underappreciated plant vulnerabilities to heat waves. *The New Phytologist*, *231*, 32–39.

Brzostek, E. R., Dragoni, D., Schmid, H. P., Rahman, A. F., Sims, D., Wayson, C. A., Johnson, D. J., & Phillips, R. P. (2014). Chronic water stress reduces tree growth and the carbon sink of deciduous hardwood forests. *Global Change Biology*, *20*(8), 2531–2539.

Bytnerowicz, T. A., Akana, P. R., Griffin, K. L., & Menge, D. N. L. (2022). Temperature sensitivity of woody nitrogen fixation across species and growing temperatures. *Nature Plants*, *8*(3), 209–216.

Canham, C. D., Murphy, L., Riemann, R., McCullough, R., & Burrill, E. (2018). Local differentiation in tree growth responses to climate. *Ecosphere*, *9*(8), e02368.

Castagneri, D., Battipaglia, G., von Arx, G., Pacheco, A., & Carrer, M. (2018). Tree-ring anatomy and carbon isotope ratio show both direct and legacy effects of climate on bimodal xylem formation in pinus pinea. *Tree Physiology*, *38*(8), 1098–1109.

Charney, N. D., Babst, F., Poulter, B., Record, S., Trouet, V. M., Frank, D., Enquist, B. J., & Evans, M. E. (2016). Observed forest sensitivity to climate implies large changes in 21st century north american forest growth. *Ecology Letters*, *19*(9), 1119–1128.

Clark, J. S. (2016). Why species tell more about traits than traits about species: Predictive analysis. *Ecology*, *97*(8), 1979–1993.

Cook, E. R. (1987). The decomposition of tree-ring series for environmental studies.

D'Arrigo, R., Wilson, R., Liepert, B., & Cherubini, P. (2008). On the 'divergence problem' in northern forests: A review of the tree-ring evidence and possible causes. *Global and Planetary Change*, *60*(3–4), 289–305.

DeRose, R. J., Shaw, J. D., & Long, J. N. (2017). Building the forest inventory and analysis tree-ring data set. *Journal of Forestry*, *115*(4), 283–291.

DeSoto, L., Cailleret, M., Sterck, F., Jansen, S., Kramer, K., Robert, E. M. R., Aakala, T., Amoroso, M. M., Bigler, C., Camarero, J. J., Čufar, K., Gea-Izquierdo, G., Gillner, S., Haavik, L. J., Hereş, A. M., Kane, J. M., Kharuk, V. I., Kitzberger, T., Klein, T., … Martínez-Vilalta, J. (2020). Low growth resilience to drought is related to future mortality risk in trees. *Nature Communications*, *11*(1), 1–9.

D'Orangeville, L., Itter, M., Kneeshaw, D., Munger, J. W., Richardson, A. D., Dyer, J. M., Orwig, D. A., Pan, Y., & Pederson, N. (2022). Peak radial growth of diffuse-porous species occurs during periods of lower water availability than for ring-porous and coniferous trees. *Tree Physiology*, *42*(2), 304–316.

D'Orangeville, L., Maxwell, J., Kneeshaw, D., Pederson, N., Duchesne, L., Logan, T., Houle, D., Arseneault, D., Beier, C. M., Bishop, D. A., Druckenbrod, D., Fraver, S., Girard, F., Halman, J., Hansen, C., Hart, J. L., Hartmann, H., Kaye, M., Leblanc, D., … Phillips, R. P. (2018). Drought timing and local climate determine the sensitivity of eastern temperate forests to drought. *Global Change Biology*, *24*(6), 2339–2351.

Dreyer, E., Le Roux, X., Montpied, P., Daudet, F. A., & Masson, F. (2001). Temperature response of leaf photosynthetic capacity in seedlings from seven temperate tree species. *Tree Physiology*, *21*(4), 223–232.

Etzold, S., Sterck, F., Bose, A. K., Braun, S., Buchmann, N., Eugster, W., Gessler, A., Kahmen, A., Peters, R. L., Vitasse, Y., Walthert, L., Ziemińska, K., & Zweifel, R. (2022). Number of growth days and not length of the growth period determines radial stem growth of temperate trees. *Ecology Letters*, *25*(2), 427–439.

Evans, M. E. K., DeRose, R. J., Klesse, S., Girardin, M. P., Heilman, K. A., Alexander, M. R., Arsenault, A., Babst, F., Bouchard, M., Cahoon, S. M. P., Campbell, E. M., Dietze, M., Duchesne, L., Frank, D. C., Giebink, C. L., Gómez-Guerrero, A., García, G. G., Hogg, E. H., Metsaranta, J., … GaytÁn, S. (2022). Adding tree rings to north america's national forest inventories: An essential tool to guide drawdown of atmospheric CO_2. *Bioscience*, *72*(3), 233–246.

Fatichi, S., Leuzinger, S., & Körner, C. (2014). Moving beyond photosynthesis: From carbon source to sink-driven vegetation modeling. *New Phytologist*, *201*(4), 1086–1095.

Frank, D., Reichstein, M., Bahn, M., Thonicke, K., Frank, D., Mahecha, M. D., Smith, P., Van der Velde, M., Vicca, S., Babst, F., Beer, C., Buchmann, N., Canadell, J. G., Ciais, P., Cramer, W., Ibrom, A., Miglietta, F., Poulter, B., Rammig, A., … Zscheischler, J. (2015). Effects of climate extremes on the terrestrial carbon cycle: Concepts, processes and potential future impacts. *Global Change Biology*, *21*(8), 2861–2880.

Fritts, H. (2012). *Tree rings and climate*. Elsevier.

Fritts, H. C. (1974). Relationships of ring widths in arid-site conifers to variations in monthly temperature and precipitation. *Ecological Monographs*, *44*(4), 411–440.

Gantois, J. (2022). Dataset supporting "new tree-level temperature response curves document sensitivity of tree growth to high temperatures across a us-wide climatic gradient".

Gaure, S. (2021). Lfe: Linear group fixed effects.

George, S. S. (2014). An overview of tree-ring width records across the northern hemisphere. *Quaternary Science Reviews*, *95*, 132–150.

Girardin, M. P., Guo, X. J., Metsaranta, J., Gervais, D., Campbell, E., Arsenault, A., Isaac-Renton, M., Harvey, J. E., Bhatti, J., & Hogg, E. H. (2021). A national tree-ring data repository for Canadian forests (cfs-trend): Structure, synthesis, and applications. *Environmental Reviews*, *29*(2), 225–241.

Gratani, L. (2014). Plant phenotypic plasticity in response to environmental factors. *Advances in Botany*, *2014*, 1–17.

Gunderson, C. A., O'hara, K. H., Campion, C. M., Walker, A. V., & Edwards, N. T. (2010). Thermal plasticity of photosynthesis: The role of acclimation in forest responses to a warming climate. *Global Change Biology*, *16*(8), 2272–2286.

Heilman, K. A., Dietze, M. C., Arizpe, A. A., Aragon, J., Gray, A., Shaw, J. D., Finley, A. O., Klesse, S., DeRose, R. J., & Evans, M. E. K. (2022). Ecological forecasting of tree growth: Regional fusion of tree-ring and forest inventory data to quantify drivers and characterize uncertainty. *Global Change Biology*, *28*(7), 2442–2460.

Hicke, J. A., Allen, C. D., Desai, A. R., Dietze, M. C., Hall, R. J., Hogg, E. H., Kashian, D. M., Moore, D., Raffa, K. F., Sturrock, R. N., & Vogelmann, J. (2012). Effects of biotic disturbances on forest carbon cycling in the United States and Canada. *Global Change Biology*, *18*(1), 7–34.

Huang, M., Piao, S., Ciais, P., Peñuelas, J., Wang, X., Keenan, T. F., Peng, S., Berry, J. A., Wang, K., Mao, J., Alkama, R., Cescatti, A., Cuntz, M., de Deurwaerder, H., Gao, M., He, Y., Liu, Y., Luo, Y., Myneni, R. B., … Janssens, I. A. (2019). Air temperature optima of vegetation productivity across global biomes. *Nature Ecology & Evolution*, *3*(5), 772–779.

IPCC. (2021). Summary for policymakers. In V. Masson-Delmotte, P. Zhai, A. Pirani, S. L. Connors, C. Péan, S. Berger, N. Caud, Y. Chen, L. Goldfarb, M. I. Gomis, M. Huang, K. Leitzell, E. Lonnoy, J. B. R. Matthews, T. K. Maycock, T. Waterfield, O. Yelekçi, R. Yu, & B. Zhou (Eds.), *Climate change 2021: The physical science basis. Contribution of working group I to the sixth assessment report of the intergovernmental panel on climate change* (pp. 3–32). Cambridge University Press.

Itter, M. S., D'Orangeville, L., Dawson, A., Kneeshaw, D., Duchesne, L., & Finley, A. O. (2019). Boreal tree growth exhibits decadal-scale ecological memory to drought and insect defoliation, but no negative response to their interaction. *Journal of Ecology*, *107*(3), 1288–1301.

Jacoby, G. C., Cook, E. R., & Ulan, L. D. (1985). Reconstructed summer degree days in Central Alaska and northwestern Canada since 1524 1. *Quaternary Research*, *23*(1), 18–26.

Kattge, J., & Knorr, W. (2007). Temperature acclimation in a biochemical model of photosynthesis: A reanalysis of data from 36 species. *Plant, Cell & Environment*, *30*(9), 1176–1190.

Klein, T. (2014). The variability of stomatal sensitivity to leaf water potential across tree species indicates a continuum between isohydric and anisohydric behaviours. *Functional Ecology*, *28*(6), 1313–1320.

Klesse, S., DeRose, R. J., Babst, F., Black, B. A., Anderegg, L. D., Axelson, J., Ettinger, A., Griesbauer, H., Guiterman, C. H., Harley, G., Harvey, J. E., Lo, Y. H., Lynch, A. M., O'Connor, C., Restaino, C., Sauchyn, D., Shaw, J. D., Smith, D. J., Wood, L., … Evans, M. (2020). Continental-scale tree-ring-based projection of Douglas-fir growth: Testing the limits of space-for-time substitution. *Global Change Biology*, *26*(9), 5146–5163.

Klesse, S., DeRose, R. J., Guiterman, C. H., Lynch, A. M., O'Connor, C. D., Shaw, J. D., & Evans, M. E. (2018). Sampling bias overestimates climate change impacts on forest growth in the southwestern United States. *Nature Communications*, *9*(1), 1–9.

Kottek, M., Grieser, J., Beck, C., Rudolf, B., & Rubel, F. (2006). World map of the köppen-Geiger climate classification updated.

Liu, Y., Kumar, M., Katul, G. G., & Porporato, A. (2019). Reduced resilience as an early warning signal of forest mortality. *Nature Climate Change*, *9*(11), 880–885.

Lloyd, J., & Farquhar, G. D. (2008). Effects of rising temperatures and [CO_2] on the physiology of tropical forest trees. *Philosophical Transactions of the Royal Society, B: Biological Sciences*, *363*(1498), 1811–1817.

Ma, S., Osuna, J. L., Verfaillie, J., & Baldocchi, D. D. (2017). Photosynthetic responses to temperature across leaf–canopy–ecosystem scales: A 15-year study in a californian oak-grass savanna. *Photosynthesis Research*, *132*(3), 277–291.

Martin-Benito, D., & Pederson, N. (2015). Convergence in drought stress, but a divergence of climatic drivers across a latitudinal gradient in a temperate broadleaf forest. *Journal of Biogeography*, *42*(5), 925–937.

McDowell, N., Pockman, W. T., Allen, C. D., Breshears, D. D., Cobb, N., Kolb, T., Plaut, J., Sperry, J., West, A., Williams, D. G., & Yepez, E. A. (2008). Mechanisms of plant survival and mortality during drought: Why do some plants survive while others succumb to drought? *New Phytologist*, *178*(4), 719–739.

McKenzie, D., Peterson, D. L., & Littell, J. J. (2008). Global warming and stress complexes in forests of western north America. *Developments in Environmental Science*, *8*, 319–337.

Medlyn, B. E., Dreyer, E., Ellsworth, D., Forstreuter, M., Harley, P. C., Kirschbaum, M. U. F., Le Roux, X., Montpied, P., Strassemeyer, J., Walcroft, A., Wang, K., & Loustau, D. (2002). Temperature response of parameters of a biochemically based model of photosynthesis. II. A review of experimental data. *Plant, Cell & Environment*, *25*(9), 1167–1179.

Melillo, J., Steudler, P., Aber, J., Newkirk, K., Lux, H., Bowles, F., Catricala, C., Magill, A., Ahrens, T., & Morrisseau, S. (2002). Soil warming and carbon-cycle feedbacks to the climate system. *Science*, *298*(5601), 2173–2176.

Montgomery, R. A., Rice, K. E., Stefanski, A., Rich, R. L., & Reich, P. B. (2020). Phenological responses of temperate and boreal trees to warming depend on ambient spring temperatures, leaf habit, and geographic range. *Proceedings of the National Academy of Sciences of the United States of America*, *117*(19), 10397–10405.

Nievola, C. C., Carvalho, C. P., Carvalho, V., & Rodrigues, E. (2017). Rapid responses of plants to temperature changes. *Temperature*, *4*(4), 371–405.

O'sullivan, O. S., Heskel, M. A., Reich, P. B., Tjoelker, M. G., Weerasinghe, L. K., Penillard, A., Zhu, L., Egerton, J. J., Bloomfield, K. J., Creek, D., Bahar, N. H. A., Griffin, K. L., Hurry, V., Meir, P., Turnbull, M. H., & Atkin, O. K. (2017). Thermal limits of leaf metabolism across biomes. *Global Change Biology*, *23*(1), 209–223.

Pachauri, R. K., Allen, M. R., Barros, V. R., Broome, J., Cramer, W., Christ, R., Church, J. A., Clarke, L., Dahe, Q., Dasgupta, P., Dubash, N. K., Edenhofer, O., Elgizouli, I., Field, C. B., Forster, P., Friedlingstein, P., Fuglestvedt, J., Gomez-Echeverri, L., Hallegatte, S., … van Ypserle, J.-P. (2014). *Climate change 2014: Synthesis report. Contribution of working groups I, II and III to the fifth assessment report of the intergovernmental panel on climate change*. IPCC.

Parent, B., Turc, O., Gibon, Y., Stitt, M., & Tardieu, F. (2010). Modelling temperature-compensated physiological rates, based on the coordination of responses to temperature of developmental processes. *Journal of Experimental Botany*, *61*(8), 2057–2069.

Patterson, A. E., Arkebauer, R., Quallo, C., Heskel, M. A., Li, X., Boelman, N., & Griffin, K. L. (2018). Temperature response of respiration and respiratory quotients of 16 co-occurring temperate tree species. *Tree Physiology*, *38*(9), 1319–1332.

Peters, R. L., Steppe, K., Cuny, H. E., De Pauw, D. J., Frank, D. C., Schaub, M., Rathgeber, C. B., Cabon, A., & Fonti, P. (2021). Turgor–a limiting factor for radial growth in mature conifers along an elevational gradient. *New Phytologist*, *229*(1), 213–229.

Poyatos, R., Aguadé, D., Galiano, L., Mencuccini, M., & Martínez-Vilalta, J. (2013). Drought-induced defoliation and long periods of near-zero gas exchange play a key role in accentuating metabolic decline of scots pine. *New Phytologist*, *200*(2), 388–401.

R Core Team. (2021). *R: A language and environment for statistical computing*. R Foundation for Statistical Computing.

Restaino, C. M., Peterson, D. L., & Littell, J. (2016). Increased water deficit decreases Douglas fir growth throughout western us forests. *Proceedings of the National Academy of Sciences of the United States of America*, *113*(34), 9557–9562.

Roman, D., Novick, K., Brzostek, E., Dragoni, D., Rahman, F., & Phillips, R. (2015). The role of isohydric and anisohydric species in determining ecosystem-scale response to severe drought. *Oecologia*, *179*(3), 641–654.

Schlenker, W., & Roberts, M. J. (2006). Nonlinear effects of weather on corn yields. *Review of Agricultural Economics*, *28*(3), 391–398.

Schlenker, W., & Roberts, M. J. (2009). Nonlinear temperature effects indicate severe damages to us crop yields under climate change.

Proceedings of the National Academy of Sciences of the United States of America, *106*(37), 15594–15598.

Schofield, M. R., Barker, R. J., Gelman, A., Cook, E. R., & Briffa, K. R. (2016). A model-based approach to climate reconstruction using tree-ring data. *Journal of the American Statistical Association*, *111*(513), 93–106.

Sitch, S., Huntingford, C., Gedney, N., Levy, P. E., Lomas, M., Piao, S., Betts, R., Ciais, P., Cox, P., Friedlingstein, P., Jones, C. D., Prentice, I. C., & Woodward, F. I. (2008). Evaluation of the terrestrial carbon cycle, future plant geography and climate-carbon cycle feedbacks using five dynamic global vegetation models (dgvms). *Global Change Biology*, *14*(9), 2015–2039.

Smith, N. G., & Dukes, J. S. (2013). Plant respiration and photosynthesis in global-scale models: Incorporating acclimation to temperature and co 2. *Global Change Biology*, *19*(1), 45–63.

StataCorp. (2019). *Stata statistical software: Release 16*. StataCorp LLC.

Steinschneider, S., Cook, E. R., Briffa, K. R., & Lall, U. (2017). Hierarchical regression models for dendroclimatic standardization and climate reconstruction. *Dendrochronologia*, *44*, 174–186.

Trugman, A. T., Anderegg, L. D., Anderegg, W. R., Das, A. J., & Stephenson, N. L. (2021). Why is tree drought mortality so hard to predict? *Trends in Ecology & Evolution*, *36*(6), 520–532.

Vicente-Serrano, S. M., Gouveia, C., Camarero, J. J., Beguería, S., Trigo, R., López-Moreno, J. I., Azorín-Molina, C., Pasho, E., Lorenzo-Lacruz, J., Revuelto, J., Morán-Tejeda, E., & Sanchez-Lorenzo, A. (2013). Response of vegetation to drought time-scales across global land biomes. *Proceedings of the National Academy of Sciences of the United States of America*, *110*(1), 52–57.

Wang, K.-Y., Kellomäki, S., & Laitinen, K. (1996). Acclimation of photosynthetic parameters in scots pine after three years exposure to elevated temperature and CO_2. *Agricultural and Forest Meteorology*, *82*(1–4), 195–217.

Waring, R. H., & Running, S. W. (2010). *Forest ecosystems: Analysis at multiple scales*. Elsevier.

Williams, A. P., Allen, C. D., Macalady, A. K., Griffin, D., Woodhouse, C. A., Meko, D. M., Swetnam, T. W., Rauscher, S. A., Seager, R., Grissino-Mayer, H. D., Dean, J. S., Cook, E. R., Gangodagamage, C., Cai, M., & McDowell, N. G. (2013). Temperature as a potent driver of regional forest drought stress and tree mortality. *Nature Climate Change*, *3*(3), 292–297.

Winkler, A. J., Myneni, R. B., Alexandrov, G. A., & Brovkin, V. (2019). Earth system models underestimate carbon fixation by plants in the high latitudes. *Nature Communications*, *10*(1), 1–8.

Yi, K., Dragoni, D., Phillips, R. P., Roman, D. T., & Novick, K. A. (2017). Dynamics of stem water uptake among isohydric and anisohydric species experiencing a severe drought. *Tree Physiology*, *37*(10), 1379–1392.

Zweifel, R., Rigling, A., & Dobbertin, M. (2009). Species-specific stomatal response of trees to drought–a link to vegetation dynamics? *Journal of Vegetation Science*, *20*(3), 442–454.

SUPPORTING INFORMATION

Additional supporting information can be found online in the Supporting Information section at the end of this article.

How to cite this article: Gantois, J. (2022). New tree-level temperature response curves document sensitivity of tree growth to high temperatures across a US-wide climatic gradient. *Global Change Biology*, *28*, 6002–6020. https://doi.org/10.1111/gcb.16313